3D Reconstruction from JPG Images

Youssif Mohamed Mostafa, Maryam N. Al-Berry, Howida A. Shedeed
Scientific Computing Department-Faculty of Computer and Information Science, Ain Shams University, Cairo, Egypt

***Abstract*—Three-dimensional (3D) reconstruction from two-dimensional (2D) images is a fundamental challenge in computer vision and photogrammetry, with applications in medical imaging, robotics, and augmented reality. This research introduces an image-based modeling pipeline designed to overcome the inherent limitations of Joint Photographic Experts Group (JPEG) images, such as lossy compression and reduced structural fidelity. The proposed hybrid framework integrates photogrammetric methods specifically Structure-from-Motion (SFM) and Dense Stereo Matching with advanced point cloud generation and surface reconstruction techniques. Initially, Marching Cubes was utilized to generate dense point clouds from sequential JPEG slices, followed by Poisson Surface Reconstruction to produce watertight 3D models. Structural details are further enhanced using Structural Similarity index (SSIM) guided texture refinement. Evaluated on the Kaggle Chest CT Segmentation dataset, the method achieves an SSIM score of 0.725, outperforming the JPEG-based reconstruction baseline of 0.675 by 7.4%. In addition to improved accuracy, the study explores the balance between computational cost and reconstruction quality, offering insights relevant to real time and resource constrained applications. By bridging photogrammetry with computer vision, this work advances practical 3D reconstruction from compressed medical images, enabling efficient digitization in low-bandwidth environments.**

Keywords*—*3D reconstruction; photogrammetry; computer vision; image-based modeling; point cloud generation; JPEG images

I. Introduction

Three-dimensional (3D) reconstruction of structures from two-dimensional (2D) images remains a persistent and challenging problem in computer vision, particularly in scenarios where direct 3D acquisition via specialized sensors is either impractical or unavailable. In the medical domain, particularly in diagnostic imaging and surgical planning, the ability to infer 3D anatomy from 2D image data is of critical importance. Classical approaches to this problem are grounded in multi-view geometry and utilize geometric relationships between multiple views to estimate depth, determine camera motion, and recover the underlying spatial structure [1], [2].

The vital components needed to create the 3D reconstructed model are the Red-Green-Blue (RGB) values and the depth map which is considered as the crucial value to reconstruct a watertight model [3]. The depth map contains the distance between the camera viewpoint and the reconstructed surface of the model.

In many clinical workflows, available datasets are stored as JPEG slices in compressed format from Computed Tomography (CT) scans. Although these images offer wide accessibility and storage efficiency, the JPEG format introduces several limitations, including lossy compression, quantization noise, structural artifacts and lack of depth information. Because the more information of the depth of each point in the point cloud, the closer the reconstructed model will be realistic and non-manifold. These issues can adversely affect key stages of the reconstruction pipeline, such as feature detection and matching, depth estimation, and surface extraction, thereby complicating the task of accurate anatomical reconstruction.

In this work, a pipeline for reconstructing 3D anatomical surfaces from JPEG-compressed CT image slices using classical computer vision techniques is proposed. The pipeline begins with robust feature detection and matching across sequential CT slices and masks, by extracting the global bounding box from the masks to extract the point of interest organ across all the CTs and crop them to the exact dimension, followed by camera pose approximation and sparse point cloud generation via SFM [4]. The sparse cloud is then densified using Multi-View Stereo (MVS) to generate a detailed volumetric representation of the anatomical region [5]. To extract a continuous and topologically coherent surface from this volumetric data, the Marching Cubes algorithm is applied [6], which constructs an initial isosurface by interpolating scalar field values across a 3D grid. For further refinement, Poisson Surface Reconstruction is employed [7], which formulates surface recovery as a spatial Poisson problem, enabling the generation of smooth, watertight surfaces that preserve geometric detail and continuity. Finally, face reduction technique is applied to reduce the number of faces and polygons in the model while maintaining a visually similar model according to the SSIM factor.

This study demonstrates that high-quality 3D reconstructions of anatomical structures can be achieved using classical methods, even when relying solely on JPEG-compressed CT images and the estimation of the depth value. The proposed pipeline is evaluated on clinical datasets, highlighting its effectiveness and the trade-offs involved in balancing reconstruction accuracy, computational efficiency, and the limitations of compressed medical imaging data.

The rest of the paper is organized as follows: Section II provides a survey on related works of 3D reconstruction. Section III explains the background and methods used. Section IV details the proposed pipeline, Section V presents the used datasets, experiments, and achieved results. Finally, section VI presents our conclusions and future work directions.

II. Related Work

Many researchers proposed several techniques to contribute to the 3D reconstruction problem either by using deep learning-based methodologies [8], [9], or classical computer vision

techniques [10], [11], [12], [13]. The following introduces a summary of the state-of-the-art methodologies that use classical and deep learning computer vision techniques, since they are more related to the proposed method.

In study [10], the authors started to collect images from the medical field, like CT images, and then improved the quality of the images. Two different methods were used to create the 3D model. The first method, called "volume rendering", was used to scan the CT and MR images. It started from one pixel and produced a steady light beam and scanned each pixel in the image. If the light source is different, the resulting image will be different. The second method, called "surface rendering", used a series of related surfaces from volumed data, and started to extract the outer lines of each slice image. The results demonstrated that the statistical model improved alignment precision and robustness and provided valuable insights for enhancing image-guided diagnosis and interventions in clinical settings.

G. Caravaca *et al.* [11] used 3D reconstruction to simulate the Kimberley outcrop on Mars. They used multiple cameras with different perspectives and camera lenses in different calculated locations to collect images of Gale crater, which contains a lot of geographical terrains. Firstly, they used the cameras that were mounted on the Mars Science Laboratory Rover, known as *Curiosity,* to capture images from Mars' surface. Secondly, they used the captured and collected images from Mars Hans Lens Imager (MAHLI). Finally, they combined the outputs from those two steps in one database. They used 2175 images from the collected images to be passed to a 3D mesh generator to generate a 3D mesh from the overlapped images. The final step was to use those mesh points as an input for a 3D reconstruction software (Agisoft)[1].

In study [12], Siyu Ren and Junhui Hou started with real-world scans like: ScanNet which were fed to Local Geometry representation to get a dense point cloud with un-oriented normal vectors. This dense point cloud was fed to geometry-aware Unsigned Distance Field (UDF) to predict the unsigned distance field, and the last step was to use Edge-based Marching Cubes to generate the output mesh.

In study [8], a method to improve the quality and resolution of CT images was proposed. The method aimed to improve diagnostic precision within the Internet of Health Things (IoHT) framework. They used Convolutional Neural Network (CNN) and 3D reconstruction and super-resolution (SR) to overcome the limitations of low-resolution CT images and make it possible to retrieve finer anatomical information for precise medical analysis. Specifically, the authors integrated a Generative Adversarial Network (GAN) with a Residual Network (ResNet) architecture to effectively upsample and refine CT images while preserving critical structural features. Experimental results demonstrate that the proposed method significantly outperforms traditional interpolation techniques, achieving superior image clarity and resolution as validated by quantitative metrics such as peak signal-to-noise ratio (PSNR) and SSIM.

[1] https://www.agisoft.com/

A. M. I. Mahmoud et al. [9] utilized endoscopic video footage capturing the arteries that supply blood from the heart to the prostate. The video frames were first preprocessed by removing distorted or low-quality images, after which a subset of 30 key frames was selected for analysis. These frames were then enhanced using Adobe Lightroom to reduce noise and improve clarity. Next, a 3D point cloud was generated from the processed frames and converted into a polygonal mesh, forming a detailed 3D model of the arterial structure. This model was used to quantitatively assess the precise volume of prostate tissue that must be removed to optimize blood flow dynamics, to improve vascular stability, and reduce blood pressure.

In study [13], the authors discussed the advancement of 3D CT imaging techniques in thoracic surgery, emphasizing the development of the Resection Process Map (RPM). Traditional 3D CT imaging provided static images, which may not accurately represent the dynamic nature of lung tissues during surgery. To address this, the RPM was developed to generate patient-specific, dynamic 3D images that simulate intraoperative anatomical changes, such as lung deformation due to traction. This semi-automatic system allowed thoracic surgeons to visualize different resection paths and high-quality surgical maps efficiently, enhancing preoperative planning and intraoperative navigation. The RPM demonstrated high accuracy in delineating vascular branches and bronchi, with a median image acquisition time of only 2 minutes, making it a valuable tool in modern thoracic surgical practices.

Recent advances in 3D reconstruction have leveraged various techniques, such as Deep Learning, to improve the quality and the reliability of the reconstructed model, but challenges persist. CNN-based method [8] Have achieved notable results using GANs to generate super-resolution images but often suffer from the lack of ground truth of the reconstructed images and rely on the GAN result image. Additionally, several works including [10] explored to use the CT images to reconstruct the 3D model regards the effect of the background of the CT on the reconstructed model. These limitations highlighted the need for more accurate approaches. In this work, an efficient pipeline that uses the segmented CT images to reconstruct a 3D model from JPG images is proposed.

III. Background and Methods

In this section, the techniques used in the proposed method are discussed.

A. Background

In this section, marching cubes, Poisson surface reconstruction, and face reduction are discussed.

1) Marching cubes algorithm: is a widely used algorithm to extract the polygonal mesh to represent the surface of 3D scalar field. The algorithm processes the voxel grid by comparing the scaler value of the each voxel's corner and the values of user-defined isovalues using a predefined table that represents the possible 256 values of all the configurations of triangle inside the cube, and the triangle of the voxel is generated when the intersection of the voxel and the

isosurface which lead to approximate the isosurface. For accurate rendering, vertex positions are interpolated along voxel edges, and surface normals are computed via gradient estimation. The key parameter which affect the result of marching cubes algorithm is the isovalue **τ,** as it affects the size of the model and the details generated. It decides the isosurface of the 3D scalar field. As the value of this level decreases (eg. 30 %), more details will be generated, and if the value of the level increases (eg.70%), fewer details will be generated and a less harsh isosurface is obtained.

2) Poisson surface reconstruction: is a powerful technique in 3D graphics that reconstructs smooth, watertight surfaces from oriented point clouds commonly acquired from 3D scanners or depth sensors. Unlike mesh-based approaches, it treats surface reconstruction as a spatial Poisson problem, interpreting input points and their normals as samples of an indicator function's gradient field. By solving this Poisson equation over an adaptive octree structure, the method derives an implicit function whose zero level set robustly defines the output surface. Key advantages include intrinsic noise resilience, efficient handling of large datasets, and topologically guaranteed results (e.g., no holes or self-intersections) [7]. These properties make it indispensable for applications demanding high fidelity, such as reverse engineering, cultural heritage digitization, and medical imaging, where accurate and complete surface models are critical. The key parameter of Poisson surface reconstruction is the depth. As the value of the depth increases, more details will be generated, but it will take more time to be rendered. If the value of the depth decreases, less details will be generated and the rendering will require less time.

3) Face reduction: is a fundamental technique in 3D modeling and computer graphics aimed at reducing the number of polygonal faces in a mesh while retaining its essential shape, visual fidelity, and structural integrity. This process, also called mesh simplification or decimation, is critical for optimizing 3D models in performance-sensitive applications such as video games, virtual reality, and real-time web rendering, where lower computational overhead and efficient memory usage are paramount. Advanced algorithms achieve this by strategically collapsing edges, merging vertices, or clustering polygons, prioritizing geometric features that contribute most to the model's silhouette and surface detail. Popular methods, including edge collapse, vertex clustering, and Quadric Error Metrics (QEM), offer distinct trade-offs: QEM preserves curvature with high accuracy, while clustering enables faster, coarser simplification. The choice of the technique depends on the target balance between computational efficiency, geometric precision, and artistic control over the final mesh [14].

IV. Proposed Method

Fig. 1 shows the architecture of the proposed method. First, pre-processing operations are applied to the input raw CT images. The next two consecutive stages to extract the surface and point cloud: a Marching Cubes stage, which is responsible for edge extraction for each image, and a Poisson Surface Reconstruction stage, which works to extract the mesh and faces from the provided edges. Finally, a face reduction step is used to remove redundant vertices and edges. The following sub-sections highlight the detailed procedure for each phase.

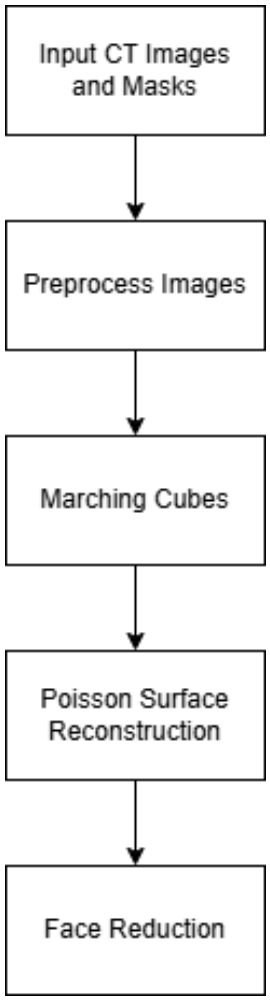

Fig. 1. The proposed annotation pipeline.

A. Preprocessing

The dataset CT images appear in the shape of (W_i, H_i, 3) Where W_i represents the width of the CT slice i, H_i represent the height of CT Slice i and 3 for the three channels of each image (red, green, blue). These input images go through a sequence of pre-processing operations as follows: as shown in Fig. 2, first each slice is processed by applying pixel-wise product with its corresponding mask to extract the image with the organ of interest (in our case the blue labeled organ in Fig. 2). Second, the bounding box is extracted for each slice by calculating its local minimum x-axis value and local maximum x-axis value and the same is done in the y-axis direction as well. The third step is to crop each slice to extract the organ image without the distortion of the background. Finally, all the images are stacked in one 3D array to be used as one unit, and this stack is in the shape of (W_i, H_i, n), where n is the number of slices.

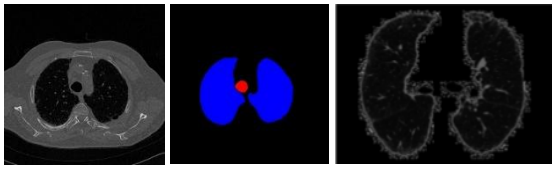

(a) (b) (c)

Fig. 2. Steps for (a) Original image, (b) Mask of the image, (c) Result image after cropping and masking.

B. Point Cloud Extraction

In this step, two algorithms are used consecutively:

1) The first is the marching cubes algorithm: The Marching Cubes algorithm is used to convert the volumetric data provided by the stacked slices into a mesh by interpolating the scalar value. It uses an iso-surface thresholding to separate the tissue of the patient organ from the background to create the surface of the organ.

2) The second algorithm is poisson surface reconstruction: The point cloud provided by the marching cubes algorithm is used to create a smooth, watertight mesh to refine the resulting surface and improve the mesh.

C. Face Reduction Step

In this step the number of the faces generated by the Poisson surface reconstruction algorithm is reduced, as shown in the results section, the number of the vertices and faces in the initial 3D model are too much to be visualize, so the number of the faces of the result model are reduced by removing the non-manifold edges, removing degenerate triangles and finally removing duplicated vertices.

V. Experimental Results

The proposed model is evaluated against a benchmark dataset, which is available on Kaggle platform.

A. Dataset

Chest-ct-segmentation[2]: The dataset consists of 16078 CT Slices and 16078 corresponding masks for a total of 114 patients. Each CT image is represented in GrayScale format while its corresponding mask is represented in RGB format. Each channel in the mask is responsible for representing a segment area for its corresponding organ. Red was used for the Trachea, blue for the Lung, and green for the Heart. In the experiments performed, only the blue channel is used as the Lungs of the patient contain a lot of details and also will be easier to visualize.

Each patient has their own number and the CTs for each patient has it's own number like: ID00323637202285211956970-1.

Three different patients were selected, and for each patient, two different organs were reconstructed from the CT scans. The selected organs were the Lung and the Heart. The IDs of the patients selected in the experiments are listed below, along with the number of CT images available in the dataset:

1) ID00323637202285211956970: 258 CT images and the corresponding 258 CT masks.

2) ID00411637202309374271828: 268 CT images and corresponding 268 CT masks.

3) ID00329637202285906759848: 260 CT images and corresponding 260 CT masks.

Each CT image is of 512×512 size, and the corresponding mask is 512×512×3 with each channel having the mask of a spacefic Organ. Fig. 3 shows sample snips from the used dataset.

B. Environmental Settings

The proposed model was implemented using Python 3.8[3] with TensorFlow 2.4 [15] backend and some helper libraries like OpenCV[4], NumPy[5], Open3D[6], scikit-image[7], scikit-learn[8], trimesh[9] and joblib[10].

The Marching Cubes algorithm is used with a level equal to 40 to capture more details and produce a richer model. Depth in the Poisson Surface Reconstruction algorithm is set to 11 to create a more detailed model, but it affects the reconstruction time. Regarding the hardware used, the system was run on Kaggle[11], which has a GPU Tesla P100, and 2 CPUs, 30 GB RAM, and 5 GB as hard drive. Finally, MeshLab[12] open-source software is used to visualize the resulting 3D model.

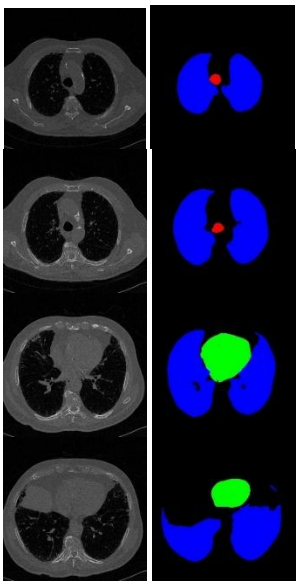

(a) (b)

Fig. 3. Samples from the Chest-CT-segmentation dataset, (a) CT images and (b) Corresponding masks.

[2] https://www.kaggle.com/datasets/polomarco/chest-ct-segmentation

[3] https://keras.io/
[4] https://opencv.org/
[5] https://numpy.org/
[6] https://www.open3d.org/
[7] https://scikit-image.org/
[8] https://scikit-learn.org/stable/
[9] https://trimesh.org/
[10] https://joblib.readthedocs.io/en/stable/
[11] https://www.kaggle.com/
[12] https://www.meshlab.net/

C. Results and Discussions

1) Experiments: In this section, the model performance is discussed. In the first experiment, we use the Marching Cubes Algorithm only and try to reconstruct the model. In the second experiment we combined the Marching cubes algorithm and Poisson Surface Reconstruction. After that we experimented the whole proposed pipeline in which we get the bounding box of the organ to reduce the size of the input image and its corresponding mask, after that we combine face reduction technique to reduce the redundant vertices and faces. Table I compares the memory cost, time cost, visual evaluation and size of the reconstructed model for the of all the experiments.

As shown in Table I, the proposed method has achieved the minimum size of the reconstructed model, as outlined in the proposed steps. First, the global bounding box of the organ from the CT image masks was extracted using its corresponding channel mask. Second, the CT bounding boxes were stacked in one stack. Third, the projection of the masks on the original CT images in the stack were used to separate the organ from the background and the resulting stack of images utilized as an input for the Marching Cubes algorithm.

TABLE I. COMPARISON RESULTS OF 3D RECONSTRUCTION

Method	Memory Cost (MB)	Time (minutes)	Size of model (MB)	Visual Evaluation
Marching Cubes	680	3	3.87	sparse representation
Marching Cubes + Poisson Surface Reconstruction	1056	7	1200	sparse representation with slice problems
Marching Cubes + Poisson surface reconstruction (with bounding box)	1214	8	400	More dense and detailed, but with a big size and redundant point problem
Marching Cubes + Poisson surface reconstruction with bounding box+ faces reduction (**Proposed**)	2680	15	12.8	Dense and detailed representation

To test the generalization of the proposed model, two different sets of experiments are performed. The first experiment is based on an EDLF-CGAN model in the data set used to extract our model, and in the second experiment the proposed model was applied on the dataset, and the results were evaluated based on peak signal-to-noise ratio (PSNR) in Eq. (1) and structural similarity (SSIM) in Eq. (3).

The PSNR is a statistical analysis indicator that is based on the gray level of image pixels, which is defined by the mean square error (MSE) in Eq. (2) between the original image I (i, j) and the reconstructed image projection from the reconstructed model K (i, j). Generally, the higher the PSNR value is, the better the image restoration is

$$PSNR = 10 \times log_{10}\left(\frac{(2^n - 1)^2}{MSE}\right) \quad (1)$$

$$MSE = \frac{1}{mn}\sum_{i=0}^{m}\sum_{j=0}^{n}\|I(i,j) - K(i,j)\|^2 \quad (2)$$

SSIM is a similarity indicator of two images. The first image is the original image, and the second is the reconstructed image projection from the reconstructed model.

$$SSIM(x,y) = \frac{(2\mu_x\mu_y + C_1)(2\sigma_{xy} + C_2)}{(\mu_x^2 + \mu_y^2 + C_1)(\sigma_x^2 + \sigma_y^2 + C_2)} \quad (3)$$

μ: Average intensity, σ: Standard deviation, σ_{xy}: Cross-correlation. C_1, C_2C_1, C_2: Stability constants.

2) Results: Table II shows the achieved results of those experiments for each patient on the lung segment against EDLF-CGAN [8]. Table III shows the achieved results of the heart segment.

TABLE II. PSNR AND SSIM ON LUNG

Model	PSNR	SSIM
EDLF-CGAN[8] (patient 1)	34.7458	0.541
EDLF-CGAN[8] (patient 2)	34.8461	0.551
EDLF-CGAN[8] (patient 3)	34.7470	0.543
Proposed (Patient 1)	36.6978	0.710
Proposed (Patient 2)	**37.1298**	**0.725**
Proposed (Patient 3)	36.6989	0.715

TABLE III. PSNR AND SSIM ON HEART

Model	PSNR	SSIM
EDLF-CGAN[8] (patient 1)	32.0021	0.422
[8] (patient 2)	32.8991	0.466
EDLF-CGAN[8] (patient 3)	32.0374	0.430
Proposed (Patient 1)	35.1347	0.632
Proposed (Patient 2)	**35.7804**	**0.675**
Proposed (Patient 3)	35.1487	0.638

As shown in Tables II and Table III, the performance of the proposed pipeline shows a significant improvement in SSIM when compared with EDLF-CGAN [8]. This is especially particularly in patient 2 as a slightly higher number of CTs and masks compared to the other patients. On the other hand, the PSNR was slightly improved with no statistically significant change. Additionally, the results of the lung show a slight increase over the heart. This is probably because the lung has a bigger reconstruction surface area and fewer structural discontinuities (such as voids or holes) in the segmentation masks.

In addition to the fact that the proposed method shows a slight enhancement in the time needed to reconstruct the model by about 27%, it also reduces the storage space used by the model by 60%. Fig. 4 shows a sample of the reconstructed models.

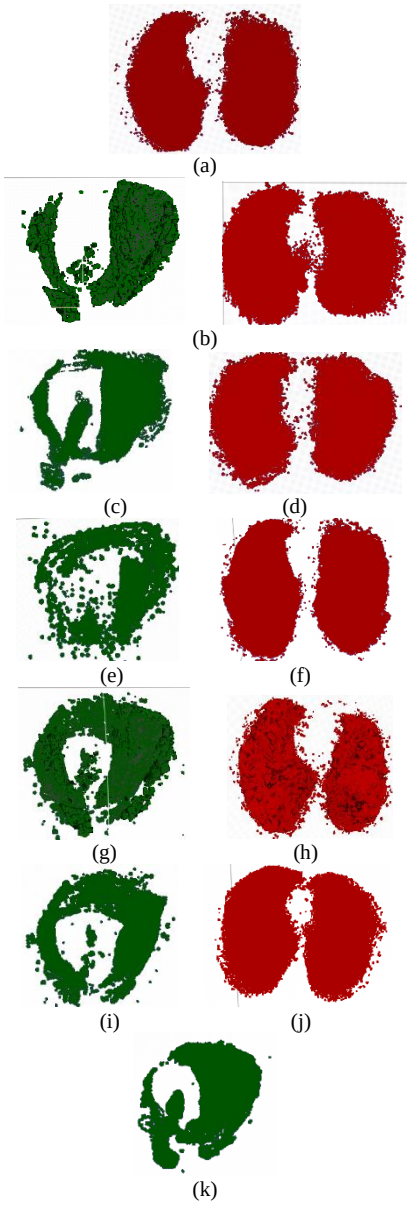

Fig. 4. Examples of models (a) Proposed patient 1 lung, (b) Proposed patient 1 heart, (c) Proposed patient 2 lung, (c) Proposed patient 2 heart, (d) Proposed patient 3 lung, (e) Proposed patient 3 heart, (f) EDLF-CGAN[8] patient 1 lung, (g) EDLF-CGAN[8] patient 1 heart, (h) EDLF-CGAN[8] patient 2 lung, (i) EDLF-CGAN[8] patient 2 heart, (j) EDLF-CGAN[8] patient 3 lung, (k) EDLF-CGAN[8] patient 3 heart.

VI. Conclusion

3D reconstruction is one of the most used fields that has become popular in recent decades. It is used in many applications like medical field applications, civil engineering field applications, games, space discovery, and urban cities reconstruction field. To avoid using learning-based models, this work proposed a traditional pipeline for three-dimensional reconstruction from JPEG-compressed computed tomography (CT) images. The proposed pipeline successfully creates precise and smooth 3D anatomical surfaces by combining Marching Cubes, Multi-View Stereo, Structure-from-Motion, and Poisson Surface Reconstruction. The suggested method shows that classical multi-view geometry and volumetric processing may produce high-quality reconstruction despite the difficulties caused by lossy compression and low depth information in JPEG photos. Results from experiments verify the pipeline's resilience and applicability for medical imaging and visualization applications, particularly when there is only compressed image data available. Even while the suggested pipeline shows encouraging outcomes when it comes to reconstructing 3D anatomical structures from JPEG-compressed CT data, there are still a number of unexplored regions. Future directions may include enhancements in the posture estimation and surface continuity accuracy by advances in feature identification and matching across very comparable CT slices. Second, the negative impacts of JPEG compression may be further reduced by including image preprocessing methods like denoising, contrast enhancement, or artifact correction. Furthermore, the method's generalizability would be enhanced by expanding its support to include additional medical imaging modalities like MRI or PET. Finally, a balance between interpretability and adaptation to intricate anatomical changes may be provided by using hybrid techniques that integrate lightweight, explainable machine learning modules with classical geometry.

References

[1] H. Ham, J. Wesley, and Hendra, “Computer vision based 3D reconstruction : A review,” International Journal of Electrical and Computer Engineering, vol. 9, no. 4, pp. 2394–2402, Aug. 2019, doi: 10.11591/ijece.v9i4.pp2394-2402.

[2] S. Speidel, S. Bodenstedt, F. Vasconcelos, and D. Stoyanov, “Interventional imaging: Vision,” Handbook of Medical Image Computing and Computer Assisted Intervention, pp. 721–745, Jan. 2019, doi: 10.1016/B978-0-12-816176-0.00034-X.

[3] P. Arbeláez, M. Maire, C. Fowlkes, and J. Malik, “Contour detection and hierarchical image segmentation,” IEEE Trans Pattern Anal Mach Intell, vol. 33, no. 5, pp. 898–916, 2011, doi: 10.1109/TPAMI.2010.161.

[4] A. Eltner and G. Sofia, “Structure from motion photogrammetric technique,” Developments in Earth Surface Processes, vol. 23, pp. 1–24, Jan. 2020, doi: 10.1016/B978-0-444-64177-9.00001-1.

[5] Y. Furukawa and C. Hernández, “Multi-view stereo: A tutorial,” Foundations and Trends in Computer Graphics and Vision, vol. 9, no. 1–2, pp. 1–148, Jun. 2015, doi: 10.1561/0600000052.

[6] J. W. Suh and Y. Kim, “Example in Computer Graphics,” Accelerating Matlab with GPUs, pp. 157–191, Jan. 2014, doi: 10.1016/B978-0-12-408080-5.00007-9.

[7] M. Kazhdan, M. Bolitho, and H. Hoppe, “Poisson Surface Reconstruction,” Eurographics Symposium on Geometry Processing, 2006.

[8] J. Zhang et al., “3D Reconstruction for Super-Resolution CT Images in the Internet of Health Things Using Deep Learning,” IEEE Access, vol. 8, pp. 121513–121525, 2020, doi: 10.1109/ACCESS.2020.3007024.

[9] A. M. I. Mahmoud, E. N. Mohamed, A. M. Tawfeek, and A. Y. Elbanhawy, “A computational approach to standardise prostatic resection interventions by virtual reconstruction,” 2021 Tenth International Conference on Intelligent Computing and Information Systems (ICICIS), pp. 413–418, Dec. 2021, doi: 10.1109/ICICIS52592.2021.9694165.

[10] J. Yao and R. Taylor, “Assessing Accuracy Factors in Deformable 2D/3D Medical Image Registration Using a Statistical Pelvis Model,” 2003.

[11] G. Caravaca, S. Le Mouélic, N. Mangold, J. L’Haridon, L. Le Deit, and M. Massé, “3D digital outcrop model reconstruction of the Kimberley outcrop (Gale crater, Mars) and its integration into Virtual Reality for simulated geological analysis,” Planet Space Sci, vol. 182, Mar. 2020, doi: 10.1016/j.pss.2019.104808.

[12] S. Ren, J. Hou, X. Chen, Y. He, and W. Wang, "GeoUDF: Surface Reconstruction from 3D Point Clouds via Geometry-guided Distance Representation," Proceedings of the IEEE International Conference on Computer Vision, pp. 14168–14178, Nov. 2022, doi: 10.1109/ICCV51070.2023.01307.

[13] T. F. Chen-Yoshikawa, "Evolution of Three-Dimensional Computed Tomography Imaging in Thoracic Surgery," Cancers 2024, Vol. 16, Page 2161, vol. 16, no. 11, p. 2161, Jun. 2024, doi: 10.3390/CANCERS16112161.

[14] D. P. Luebke, "A developer's survey of polygonal simplification algorithms," IEEE Comput Graph Appl, vol. 21, no. 3, pp. 24–35, 2001, doi: 10.1109/38.920624.

[15] R. H. Byrd, G. M. Chin, J. Nocedal, and Y. Wu, "Sample size selection in optimization methods for machine learning," Math Program, vol. 134, no. 1, pp. 127–155, Aug. 2012, doi: 10.1007/S10107-012-0572-5.